Photoluminescent road coatings for open-graded and dense-graded asphalts: a theoretical and experimental investigation

Photo-luminescent road coatings for open-graded and dense-graded asphalts: a theoretical and experimental investigation

F.G. Praticò
University Mediterranea of Reggio Calabria, Italy

R. Vaiana (*)
University of Calabria, Arcavacata Campus (CS), Italy

S. Noto
University Mediterranea of Reggio Calabria, Italy

ABSTRACT: Road safety builds on traffic and driver-infrastructure interaction: night-time visibility represents a key-aspect of this complex interaction. Therefore, providing an adequate road lighting system and improving drivers' visibility in night-time conditions is vital. In this sense, photo-luminescent paints for pavements can improve road safety in terms of visibility. The aim of the study reported here is the modelling of photo-luminescent phenomenon by referring to dense-graded (DGFC) and open-graded friction courses (OGFC), and the evaluation of the effects due to season. Measurements, based on photometry technique, were carried out in laboratory on cores. The photo-luminescent phenomenon was investigated in terms of charge and discharge time linked to decay phenomena and modelled as a function of pavement type and paint treatments. Results highlight that photo-luminescent performance depends on the luminance time and volumetric characteristics of bituminous mixtures. Results can benefit both researchers and practitioners and can allow optimising painting treatments for different bituminous mixtures.

KEYWORDS: Photoluminescent paints, friction course, luminance.

1 INTRODUCTION

Photo-luminescent materials, applied to road pavements, can help improve road safety and have more efficient markings. In more detail, bicycle paths, exit routes, parking areas can benefit because of the increase of safety during the dark hours.

Smart Highways by Dutch companies are developing photo-luminescent paints that can glow for up to 10 h at night, lighting up the roads at no cost (Rojas-Hernandez et al. 2017) (Praticò et al. 2016).

It is noted that, based on in-depth analyses and on the improvements of technical performance over time, this type of "renewable" and quite inexpensive "source" of light and traffic safety could enhance markings effectiveness (Giuliani and Autelitano 2014)

Additionally, photo-luminescent materials can counteract urban heat island effects (Okada 2015)

In order to accomplish a positive effect in terms of safety, environmental impacts, and sustainability (Cafiso and D'Agostino 2016), it is relevant to consider and to quantify both advantages (e. g., luminance effects, (Khan et al. 1999)) and disadvantages (e.g., texture decay, see (Khan et al. 1999), and friction decrease, (EN 1436:2008)), for both traditional (DGFCs) and innovative friction courses (OGFCs or similar permeable solutions). Particularly, permeable paving surfaces (such as the OGFCs) can affect strongly urban climate and this implies that assessing their overall performance is becoming more and more relevant (Santamouris 2013).

To this end, luminance is a key-factor (see Table 1). Luminance is defined by the equation 1 in Table 1, as well as Luminous flux, Φ_v, Illuminance, E, and Luminance Contrast, C.

INSERT Table 1, please

In terms of illuminance (E, see Table 1) 3 lx is considered the minimum level for night-time visibility in many traffic safety applications (Andre and Owens 2001), while values around 300 lx are commonly experienced in many interior lighting applications.

Different materials can be used for marking road pavements, such as paint, tape and spray (Andrady 1997) (Bahar et al. 2006) (Gates at al. 2003) (Jiang 2008) (Migletz and Graham 2002)

(PD 2004) (Praticò et al. 2016). The required characteristics of markings include skid resistance (Harlow 2005), reflection (in daylight or under road lighting), retroreflection (under vehicle head lamp illumination), and colour.

For illuminance (E), Table 2 illustrates how E varies as a function of the illuminating source.

INSERT Table 2, please

Note that illuminance does not depend on the surface type. Illuminance is the total amount of visible light illuminating a point on a surface from all directions above the surface and can be measured through a Lux-Meter. Instead, luminance (L) depends on surface type and (if any) on illuminating source (lux), see Table. 3. Luminance is the so-called luminous flux density in a particular direction and corresponds to the object brightness. The unit for luminance is cd/m^2 or NIT (1 NIT = 1 cd/m^2 = 1 lumen/per steradian *per* m^2 of surface).

Given that the light illuminating a surface is reflected to all angles in the same way, the on-the-surface measured illuminance (e.g., 1 lux) is more than the measured luminance of the reflected light in only one direction (e.g., 0.32 cd/m^2). Indeed, assuming a perfect diffuse reflecting surface, one can multiply the measure in cd/m^2 times π to get the equivalent value in Lux.

INSERT Table 3, please

In the pursuit of improving luminance for road safety, photo-luminescent applications are growing in interest.

Photoluminescence is the emission of visible light from anybody due to the excitement after the absorption of radiation (Oleari 2015).

Phosphorescence is a form of photoluminescence. Contrary to fluorescence (the other form of photoluminescence), phosphorescence releases absorbed radiation more slowly. It is caused by the forbidden energy state transition in quantum mechanics.

Photo-luminescent paints usually contain the following components:

- n-Butyl acetate, also known as butyl ethanoate, is an ester which is a colourless flammable liquid at room temperature.
- Xylene, which is an aromatic hydrocarbon mixture consisting of a benzene ring with two methyl groups at various substituted positions.
- Ethylbenzene, which is an organic compound, an aromatic hydrocarbon with the formula C6H5CH2CH3. It is a highly flammable, colourless liquid with an odour similar to that of gasoline.

Strontium aluminate is a solid odourless, non-flammable, pale yellow, monoclinic crystalline powder, heavier than water. It is chemically and biologically inert. When activated with a suitable dopant (e.g. europium, then it is labelled SrAl2O4:Eu), it acts as a photo-luminescent phosphor with long persistence of phosphorescence. It is used in exit signs, pathway marking, and other safety related signage (Zitoun et al. 2009).

As above mentioned, in phosphorescence, energy is absorbed and released in the form of light (photons).

If the phosphorescence quantum yield (the ratio between the number of times an event occurs and photons absorbed) is high, the release of light is significant over the time.

Energy is usually absorbed in terms of solar radiation, even if also street light can contribute.

To this end, there is a lack of information about how photo-luminescent treatments impact DGFC and OGFC surface properties and luminance.

2 OBJECTIVES

The main objectives of this study are: i) to model the photo-luminescent phenomenon (release) with regard to both dense-graded and open-graded friction courses; ii) to assess surface modifications (friction and texture) due to paint application.

3 PROCEDURES AND EXPERIMENTS

In order to pursue the objectives above: a) a primer was used (white paint, WP); b) a phosphorescent paint was laid on the primer (PP); c) charge and discharge time was assessed to model the phenomenon; d) texture tests were carried out (by means of a laser scanner). In more detail, experimental investigation was carried out according to the scheme shown in Fig. 1 and was organized into the following main tasks:

1. On site compaction of DGFC and OGFC and photo-luminescent material selection;
2. Cores extraction and testing before painting (surface texture spectrum, (ISO/CD TS 13473-4: 2008) (ISO 13473-1: 1997); surface friction (EN 13036-4: 2011) (Praticò and Astolfi 2017);
3. Cores painting;
4. Cores testing after painting;
5. Luminance measurements, carried out in daylight hours and in night-time conditions, both in summer and winter. A photometer was used.
6. Data analysis;
7. Modelling of the luminance phenomenon.

Note that tests were carried out in the laboratory under controlled conditions while treatments were preliminary set up on site.

INSERT Figure 1, please

This research was developed considering two different types of wearing course: Open Graded Friction Courses (OGFC) and Dense Graded Friction Courses (DGFC).

OGFCs and DGFCs were tested for air voids content (Praticò and Moro 2011) (Praticò et al. 2013a) (Praticò and Vaiana 2013b). OGFCs air voids content was 25-28% before paint application and 22-24% after, while for DGFCs it was 5-12% before and 5-11% after (Praticò et al.

114 2015).

115 Also friction was investigated in terms of British Pendulum Number (BPN) (EN 13036-4:
116 2011). In particular, BPN for OGFCs was 46-62 before paint application and 21-31 after; while,
117 for DGFCs, BPN was 56-64 before and 10-21 after paint application.

118 The samples used for the investigation were treated with two paints: a white paint (used like a
119 primer) and a phosphorescent paint. Timing and quantities for the application of the paint were
120 established according to the specification sheet provided by the manufacturer (Tab. 5) and based
121 on previous investigations (Praticò et al. 2016). A drain down effect was noted for OGFCs.

122 Texture surveys were structured as shown in Fig. 2.

123 The surface of the samples was characterized in terms of surface texture both before and after
124 coating the paint.

125 In particular, a measurement was performed, by a laser profilometer, based on conoscopic ho-
126 lography.

127 The device above has the following characteristics (ISO 13473-3: 2002) (Praticò et al. 2014):
128 i) Mobility: stationary, slow (time on lane per single measurement equal or higher than 1 mi-
129 nute); ii) Texture wavelength range: range covered BD class 0.20÷50mm; iii) Pavement contact:
130 contactless devices; iv) Principle of operation: laser profilometer; v) Objective focal length:
131 100mm; vi) Max vertical measuring range: 35mm; vii) Vertical resolution for class 0.003÷0.03
132 mm: 0.012mm; viii) Stand-off distance: 90mm; ix) Minimum horizontal resolution Δx (sam-
133 pling interval) BD for class 0.05÷1 mm: 0.01mm; x) Angle coverage: 170°.

134 For each sample, three profiles (i, j, k, 120 degrees far) were measured, (see Fig. 2).

135

136 **INSERT Figure 2, please**

137

138 Note that, due to core diameter (100mm), the highest wave length was 10mm (λ_{max} =
139 100mm/10).

140 Table 4 lists the main indicators derived based on sample profiles (three profiles per samples,

see (ISO 13473-1: 1997) (ISO 13473-3: 2002) (EN 13036-4: 2011) (Boscaino and Praticò 2001) (Praticò and Moro 2011) (Praticò et al. 2013a) (Praticò and Vaiana 2013b) (Praticò et al. 2014) (Praticò et al. 2015) (Praticò and Astolfi 2017).

The main steps of data treatment were as follows: (i) interpolation of drop-outs; (ii) offset and slope suppression; (iii) windowing (a Hanning window and the profile $Z_{i,\ win}$ was used) and (iv) Fast Fourier Transform implementation.

INSERT Table 4, please

INSERT Table 5, please

4 MODELING

Cycles were modelled as in Fig. 3, in terms of charge (C) and discharge (D) phase, charge and discharge slope (CS, DS), charge and discharge time (CT, DT), and luminance time (t_L<DT).

INSERT Figure 3, please

Based on the above and based on the study of the data, the following luminance curve is here-in set up (night-time discharge):

$$L = a \cdot t^b \tag{7}$$

where L is luminance (cd/m^2), t is time (s), a and b are coefficients to calibrate.

Note that in Fig. 3 the following points are indicated (out of scale): D_1, D_2, D_3.

In order to make the regression curve of equation (7) consistent, the following notes apply:

- The abscissa of D_1 is the time t_1 at which the luminance has the highest value measured in the

given cycle:

$$t_1 = \left(\frac{L_{\max}}{a} \right)^{1/b} \tag{8}$$

- The abscissa of D_2 is the time t_L at which the luminance approaches the threshold value (0.01 cd/m^2):

$$t_2 = \left(\frac{0.01}{a} \right)^{1/b} \tag{9}$$

- The difference t_2-t_1 is the conventional luminance time t_L:

$$t_L = t_2 - t_1 \tag{10}$$

Consequently, t_L time, so that $L(t_L)$=0.01 cd/m^2, is derived. As described, note that 0.01 corresponds to a sort of threshold at which the central visual system does not support high acuity or colour vision (Bullought et al. 2014) (Deng et al. 2005) (Rea et al. 2004).

Under the abovementioned hypotheses, the average value of luminance in t_1, t_2 is herein derived as follows:

$$L_M = \frac{\int_{t_2}^{t_1} a x^b dx}{t_L} = a \frac{x^{b+1}}{(b+1) t_L} \Bigg|_{t_1}^{t_2} \tag{11}$$

The average slope in the period (t_1, t_2), that is to say D_2-D_1, is:

$$DS = \frac{\int_{t_2}^{t_1} y' dx}{t_L} = \frac{\int_{t_2}^{t_1} abx^{b-1} dx}{t_L} = \frac{ab}{t_L} \frac{x^{b-1+1}}{b-1+1} \Bigg|_{t_1}^{t_2} = \frac{ax^b}{t_L} \Bigg|_{t_1}^{t_2} \tag{12}$$

Based on the above facts, the following performance indicator, PI, is herein defined:

$$PI = \int_{t_2}^{t_1} ax^b dx = a \frac{x^{b+1}}{b+1}\Bigg|_{t_1}^{t_2} \tag{13}$$

Based on the model above set up, L_M represents the average luminance, while DS provides information on how fast is the decay. Finally, PI represents the performance of the treatment because it considers both the duration and the luminance. Note that the three indicators above are applied to both literature (Tab. 6) and data obtained (Cf. Figures 14 and 15).

It is worth noting that the response of a given treatment depends on the energy absorbed.

This latter depends on a number of factors, among which the following can be listed:

Solar constant (1367 W/m^2), day of the year (N), cosine effect (θ_z, which depends on latitude). Overall, it turns out that the direct radiation (kW/m^2) is a curve which is approximatively zero between sunset and sunrise and has a value in the range 0~1 kW/m^2 from dawn to sunset. Solar insolation (W·s/m^2) is the total amount of energy deposited on a surface over a period of time. It is derived by integrating (or summing) solar irradiance over that period of time. This sum is called solar radiation and has the units of energy per unit area (J/m^2 or Btu/ft^2). The daily extra-terrestrial solar radiation on a horizontal surface $H_{o,h}$ (J/m^2) can be calculated from the instantaneous values of extra-terrestrial solar irradiance, $\mathbf{I_o}$.

$$H_{o,h} = \int_{sr}^{ss} I_{o,h} dt = \int_{sr}^{ss} \left\{ I_{sc} \left[1 + 0.034 \cdot \cos\left(\frac{360N}{365.25} \right) \right] \cdot \cos\theta_z \right\} dt \tag{14}$$

where t (in seconds) is evaluated from sunrise (sr) to sunset (ss) (about 10:17 ÷ 11:20 hours in Reggio Calabria). Consequently it is approximately 33MJ/m^2.

5 RESULTS

Fig. 4 to Fig. 16 and Table 6 summarize results and analyses.

Note that the following main parameters were investigated and/or controlled:

- Typology of hot mix asphalt (open-graded or dense-graded);

- Quantity of white paint (WP) and phosphorescent paint (PP);
- Solar radiance (W/m^2);
- Cycle of charge-discharge (Charge Time, CT; Discharge Time, DT; luminance time, t_L);
- Surface Texture (Before/after);
- Seasonality aspects in terms of luminance measured;
- Other minor boundary conditions.

Fig. 4 and Fig. 5 illustrate how non-spectral indicators (MPD, Rz, RMS, Fig.4) and spectral indicators (Fig. 5) vary as a result of paint application (PP), for dense-graded (DGFC) and open-graded (OGFC) hot mix asphalt.

INSERT Figure 4, please

INSERT Figure 5, please

Based on Fig. 4 and Fig. 5, it follows that:

- OGFCs undergo higher variations in terms of non-spectral indicators; DGFCs are less affected, probably because of their negligible macrotexture;
- Rz proves to be the indicator that is most affected by paint application;

The texture levels of OGFCs yield high variability in the domain of macrotexture, while, for DGFCs, skid resistance results reduced by a factor of six.

Note that the application of white and phosphorescent paints was carried out according to Table 5.

Solar radiance, SR, is plotted in Fig. 6, Fig.7, and Fig. 8. SR is the theoretical solar radiance derived through predictive equations (which are based on the equation of the sun's position in the sky throughout the year, (Praticò et al. 2016)).

Fig. 6 illustrates the variation over time of solar radiance in summer (dotted line) and winter (solid line). Note that the peaks are lower in winter of about 0.2 kW/m^2. Fig. 7 and Fig. 8 show the night-time luminance (Ln, right y-axis, mcd/m^2) in the same days.

INSERT Figure 6, please

INSERT Figure 7, please

INSERT Figure 8, please

Table 6 and Fig. 9 illustrate how the model set up above (i.e., equations 1-13) applies to the international literature. In practice, after t_1 seconds the luminance moves towards its maximum (e.g., 18.40 cd/m^2). Afterwards, luminescence decays and at t_2 it approaches a given minimum threshold (0.01 cd/m^2). For a given L_{max}, the higher the decay time (t_2-t_1) is, the lower the slope (DS) is, the more effective is the photo-luminescence effect. Finally, PI, based on equation (13), provides an indicator of the overall effect.

INSERT Table 6, please

Importantly, model highlights that two different treatments whose performance is considered similar may exhibit high differences in terms of average. Indeed, in the case of the treatment PP on steel (Bullought et al. 2014), an average of 0.08 cd/m2 is obtained, versus about one eight of the same value when the treatment PP on illustration board (Bacero et al. 2015) is considered. Table 6 points out that the rationale behind this observation is that steeper slopes can make the treatment less competitive in spite of high initial values. Importantly, the algorithm of equation (13) considers the balance between peaks and slope characteristics. Consequently, it accomplishes the target of having an efficient representation of a sample performance.

Figures below illustrate the results and the analyses carried out in terms of the above indicators. Fig. 9 and Fig. 10 focus on the coefficients *a* and *b* (eq.7), Fig.11 and 12 illustrate how L_{max} and t_L vary (Cf. eq.10), while Fig.13 and Fig. 14 refer to discharge and averages (equations 11 and 12). Finally, Fig.15 and Fig. 16 deal with performance indicators (eq. 13), and efficiency (PI/DI, where DI is the average daily energy absorbed).

INSERT Figure 9, please

INSERT Figure 10, please

INSERT Figure 11, please

INSERT Figure 12, please

INSERT Figure 13, please

INSERT Figure 14, please

INSERT Figure 15, please

INSERT Figure 16, please

In summarising, DGFCs yield trends with better performance than OGFCs:

- Maximum luminance (L_{max}) is about twice-three times the one of OGFCs;
- Luminance time (t_L) is higher, in other words DGFCs show a longer luminance effectiveness;
- Average luminance is consistent with L_{max};
- Performance indicator, PI, as *per* the definition stated above, is, therefore, higher for DGFCs.

Based on Fig. 9 and Fig.10, it may be observed that OGFCs have higher *b*s and lower *a*s and this fact implies that photoluminescence is more persistent for DGFCs than for OGFCs (as depicted in Fig. 15 and Fig. 16). The parameter *a* (in practise, L(1s)) of DGFCs is much higher than the one of OGFCs.

On the basis of the maximum value of luminance (L_{max}), of luminance time (t_L), of average slopes (Ds), and efficiency (PI/DI), it follows that DGFCs are much more efficient then OGFCs, by a ratio of 3~8.

6 CONCLUSIONS

Based on the facts and observations above the following conclusions may be drawn:

1) Measurements suggest that the paint applied to the surface of OGFCs gradually flows inside the core voids (draindown effect). Consequently there is a limit of paint that can be applied. Surface texture (throughout the entire range of wavelengths investigated), skid resistance (which affect road safety), and pavement drainability (which impacts safety in wet condition) undergo a shift towards lower, insufficient values.
2) Samples, either OGFCs or DGFCs, show a quite similar discharge slope for all cycles.
3) Boundary conditions influence discharge time. Results show how moonlight and street light provide a kind of continuous charging.

Furthermore, based on the results obtained for OGFCs (≈ 0.02 cd/m^2) and for DGFCs (≈ 0.05 cd/m^2), it is possible to observe that:

4) The luminance of photo-luminescent bituminous surfaces is quite low. OGFCs and DGFCs yield a luminance which is similar to the one exhibited by a surface illuminated by full moon on a clear night (Schlyter 2010) (Bunning and Moser 1969);
5) A perfect diffuse reflecting surface illuminated by just 0.1-1 lux would have a luminance similar to the photo-luminescent surfaces under investigation. This corresponds to about one percent of what can be measured for an office desk.

Based on the above, it seems possible to point out that this study makes several contributions to the literature. First, this study adds to the relatively small amount of research that examines whether macrotexture and friction vary and how due to these surface treatments.

Second, the results of this study help provide a better understanding of the importance and the criticalities of assessing actual photo-luminescent performance.

Whereas previous research provides evidence that dense-graded surfaces can be easily treated, this study reveals that OGFCs applications can result unsatisfactory

Finally, evidence of algorithms to critically assess the actual performance may be of interest to practitioners and researchers.

REFERENCES

- AGO (2005). Australian Greenhouse Office. 2005. Chapter 5: Assessing lighting savings, Working Energy Resource and Training Kit: Lighting.
- Andrady, A. L. (1997). Pavement Marking Materials: Assessing Environment-Friendly Performance, NCHRP Report 392, Washington, D.C., Transportation Research Board.
- Andre, J., Owens D.A. (2001). The twilight envelope: A user-centered approach to describing roadway illumination at night. Human Factors, 43(4): 620-630.
- Austin, R.L., and Schultz, R.J. (2009). Guide to Retroreflection Safety Principles And Retroreflective Measurements, RoadVista, San Diego, California.
- Bacero, R., To, D., Arista, J.P., Dela Cruz, M.K., Villaneva, J.P., Uy, F.A. (2015). Evaluation of Strontium Alu-

minate in Traffic Paint Pavement Markings for Rural and Unilluminated Roads. 11th International Conference of Eastern Asia Society fir Transportation Studies, EASTS 2015, September 11-14, 2015, Cebu, Philippines.

- Bahar, G., Masliah, M., Erwin, T., Tan, E. and Hauer, E. (2006). Pavement Marking Materials and Markers: Real-World Relationship Between Retroreflectivity and Safety Over Time. NCHRP Web Only Document 92, Transportation Research Board.

- Boscaino, G., Praticò, F.G.. (2001). Classification et inventaire des indicateurs de la texture superfi-cielle des revetements des chausses/A classification of surface texture indices of pavement surfaces, Buletin des Laboratoires des Ponts et Chaussees, Vol. 234, pages 17-34.

- Bullough, J.D., Skinner, N.P., Snyder, J.D., Besenecker, U.C. (2014). Nighttime Highway Construction Illumination, SPR Research Study No. C-08-14, Final Report.

- Bunning, E., and Moser, I. (1969). Interference of moonlight with the photoperiodic measurement of time by plants, and their adaptive reaction, Proceedings of the National Academy of Sciences of the United States of America, vol. 62 (4), pages: 1018–1022, doi:10.1073/pnas.62.4.1018.

- Cafiso S., D'Agostino C. (2016). Assessing the stochastic variability of the Benefit-Cost ratio in roadway safety management. Accident Analysis and Prevention 93 (2016) 189–197. https://doi.org/10.1016/j.aap.2016.04.027;

- Deng, L., Chen, L., Rea, M.S. (2005). An evaluation of the Hunt94 color appearance model under different light sources at low photopic to low mesopic light levels. Color Research and Application, 30(2): 107-117.

- EN 1436: 2008. Road marking materials - Road marking performance for road users.

- EN 12464-1: 2011. Light and lighting - Lighting of work places - Part 1: Indoor work places.

- EN 13036-4: 2011 - Road and airfield surface characteristics - Test methods - Part 4: Method for measurement of slip/skid resistance of a surface: The pendulum test;

- Gates, J. T., Hawkins G.H, and Rose, E. R. (2003). Effective Pavement Marking Materials and Applications for Portland Cement Concrete Roadways2, FHWA/TX-03/4150-2, Texas Transportation Institute.

- Giuliani F., Autelitano F. (2014). "Revêtements routiers photoluminescents: étude expérimentale préliminaire en laboratoire - photoluminescent road surface dressing: a first laboratory experimental investigation", Matériaux & Techniques, 102 6-7 (2014) 603. https://doi.org/10.1051/mattech/2014030;

- Harlow, A. (2005). Skid resistance and pavement marking materials. The New Zealand Road markers Federation Inc.

- ISO 13473-1: 1997. Characterization of Pavement Texture by Use of Surface Profiles. Part 1: Determination of

Mean Profile Depth.

- ISO 13473-3: 2002. Characterization of pavement texture by use of surface profiles -- Part 3: Specification and classification of profilometers.

- ISO/CD TS 13473-4: 2008. Characterization of pavement texture by use of surface profiles — Part 4: Spectral analysis of surface profiles.

- Jiang, Y. (2008). Durability And Retro-Reflectivity Of Pavement Markings (Synthesis Study), Joint Transportation Research Program, FHWA/In/Jtrp-2007/11.

- Khan M. et al. (1999). Influence of Pavement Surface Characteristics on Nighttime Visibility of Objects. Transportation Research Record: Journal of the Transportation Research Board, Volume 1692, pp. 39-48, DOI: 10.3141/1692-06;

- Migletz, J. and Graham, J. (2002). Long-Term Pavement Marking Practices. A Synthesis of Highway Practice, NCHRP Synthesis 306, Washington, D.C., Transport Research Board of the National Academies.

- MIT 1992. Ministero delle Infrastrutture e dei Trasporti, D.Lgs. n. 285 e ss.mm.ii., 1992. Codice della Strada, Art. 2.

- Okada, J. (2015). Lotus ceramics for counteracting urban heat island effects, Eco-Efficient Materials for Mitigating Building Cooling Needs Design, Properties and Applications, 195-213.

- Oleari, C., (2015). Standard Colorimetry: Definitions, Algorithms and Software, ISBN: 978-1-118-89444-6

- OSHA (2009). Occupational Safety and Health Administration (2009), US Dept. of Labor. Illumination. - 1926.56, 2009, Regulations (Standards - 29 CFR).

- Praticò F.G., Noto S., Moro A. (2016). Optimisation of photoluminescent painting treatments on different surface layers. Functional Pavement Design - Proceedings of the 4th Chinese-European Workshop on Functional Pavement Design, CEW 2016, Delft. Erkens et al. (Eds) © 2016 Taylor & Francis Group, London, ISBN 978-1-138-02924-8

- PD 2004. Paints Directive 2004/42/EC.

- Praticò F. and Moro A. (2011). In-lab and on-site measurements of hot mix asphalt density: convergence and divergence hypotheses, "Construction and building materials", n. 25, 2011, pp. 1065-1071, https://doi.org/10.1016/j.conbuildmat.2010.06.071

- Praticò F., Vaiana R., Giunta M. (2013a), Pavement sustainability: Permeable wearing courses by recycling porous European mixes, Journal of Architectural Engineering, 19 (3), pp. 186-192,

https://10.1061/(ASCE)AE.1943-5568.0000127

- Praticò, F.G. and Vaiana, R. (2013b). A study on volumetric versus surface properties of wearing courses, Construction and Building Materials, 38: 766-775, https://10.1016/j.conbuildmat.2012.09.021

- Praticò, F, Vaiana, R, Fedele, R.. (2014). A study on the dependence of PEMs acoustic properties on incidence angle, International Journal of Pavement Engineering, https://10.1080/10298436.2014.943215 .

- Praticò F.G. and Vaiana R (2015). A study on the relationship between mean texture depth and mean profile depth of asphalt pavements. Construction & Building Materials, vol. 101, p. 72 -79, ISSN: 1879-0526, https://10.1016/j.conbuildmat.2015.10.021

- Praticò F.G., Vaiana R, Iuele T. (2015). Macrotexture modeling and experimental validation for pavement surface treatments. Construction & Building Materials, vol. 95, p. 658-666 , ISSN: 1879-0526, https:// 10.1016/j.conbuildmat.2015.07.061

- Praticò F.G. and Astolfi A., (2017). A new and simplified approach to assess the pavement surface micro- and macrotexture. Construction and Building Materials, 148 (2017), pp. 476-483. https://doi.org/10.1016/j.conbuildmat.2017.05.050

- Pears, A. (1998). Chapter 7: Appliance technologies and scope for emission reduction, Strategic Study of Household Energy and Greenhouse Issues, Sustainable Solutions Pty Ltd (Department of Industry and Science, Commonwealth of Australia), page 61.

- Rea, M.S., Bullough, J.D., Freyssinier, J.P., Bierman, A. (2004). A proposed unified system of photometry. Lighting Research and Technology, 36(2): 85-111.

- Riccardi C., Cannone Falchetto A., Losa M., Wistuba M. (2016). Back-calculation method for determining the maximum RAP content in Stone Matrix Asphalt mixtures with good fatigue performance based on asphalt mortar tests. Construction and Building Materials, Volume 118, 15 August 2016, Pages 364-372. doi: 10.1016/j.conbuildmat.2016.05.086

- Rojas-Hernandez R.E. et al., (2017). Long lasting phosphors: SrAl2O4: Eu, Dy as the most studied material. Renewable and Sustainable Energy Reviews, in press. https://doi.org/10.1016/j.rser.2017.06.081;

- Santamouris M., (2013). Using cool pavements as a mitigation strategy to fight urban heat island. A review of the actual developments. Renewable and Sustainable Energy Reviews, Volume 26, October 2013, Pages 224-240, https://doi.org/10.1016/j.rser.2013.05.047.

- Schlyter, P. (2010). Radiometry and photometry in astronomy.

- UNI 11248: 2012. Illuminazione stradale - Selezione delle categorie illuminotecniche.

- UNI EN 13201-2: 2016. Illuminazione stradale - Parte 2: Requisiti prestazionali.
- Waynant, R.W. and Ediger M.N. (2000). Electro-Optics Handbook, McGraw-Hill Professional; 2 edition.
- Zitoun, D., Bernaud, L., Manteghetti, A. (2009). Microwave Synthesis of a Long-Lasting Phosphor, J. Chem. Educ., 2009, Vol. 86, page 72

LIST OF TABLES

Table 1. Basics for estimating the effect of phosphorescent paints

Symbol and explanation	Formula		Reference value
L (cd/m^2): Luminance, the intensity of brightness and is measured in candela per unit area of a surface	$L = \frac{d^2\Phi}{dA\ d\Omega\ \cos\theta}$	(1)	1 (*)
	$L = E\rho / \pi$	(2)	
Φ (lm): Luminous flux or luminous power, measured in lumen, lm	$\Phi = V \times W$	(3)	1250 (**)
E (lx): Illuminance (E), the measure of how much luminous flux is spread over a given area or luminous power incident on a surface, S. It is measured in lx.	$E = \frac{d\Phi}{dS}$	(4)	3.4 (***)
C (dimensionless): Luminance contrast (Threshold increment)	$C = \lvert L_t - L_b \rvert / L_b$	(5)	10 (****)
R_L: Coefficient of retroreflected luminance is the most commonly used measurement of retroreflectance in highway marking. R_L is the ratio of luminance (L) of a surface to the normal illuminance (E)(Austin and Schultz 2009). Chromaticity, is the quality of a colour and it does not depend on its luminance. It consists of two parameters, hue and colourfulness.	$R_L = \frac{L}{E}$	(6)	100 (*****)

Symbols. C: luminance contrast; A: area (m^2); Ω: solid angle (sr); θ: angle between the normal to the surface and the specified direction; ρ: reflectance; V: luminous coefficient; W: luminous energy; L_t: the luminance (cd/m^2) of the target or object to be seen; L_b: the luminance (cd/m^2) of the target's or object's background;
lm: lumen; cd: candela; sr: steradian or square radian (SI unit of solid angle; a full sphere has a solid angle of 4π steradians); m: meter; lx: lux.
Notes. (*): dark limit of civil twilight under a clear sky (Waynant and Ediger 2000); (**): luminous flux of a common 18W fluorescent lamp; (***): illuminance (Tab. 2); (****): contrast value of a motorway (UNI 11248:2012); (UNI EN 13201-2:2016) classified like road of category A according to the Italian Road Classification (MIT 1992); (*****): minimum value of the coefficient of retroreflected luminance for white road markings in dry conditions (EN 1436:2008); 1 lm = 1 cd·sr; 1 lx = 1 lm/m^2 = 1 cd·sr/m^2.

Table 2. A brief comparison of illuminance values.

Surfaces illuminated by:	E [lux]
Moonless, overcast night sky (starlight) (Schlyter 2010)	0.0001
Moonless clear night sky with airglow (Schlyter 2010)	0.002
Full moon on a clear night (Bunning and Moser 1969) (Schlyter 2010)	0.27–1.00
Dark limit of civil twilight under a clear sky (Waynant and Ediger 2000)	3.40
Family living room lights (Pears 1998)	50
Office building hallway/toilet lighting (AGO 2005)	80
Very dark overcast day (Schlyter 2010)	100
Office lighting (EN 12464-1) (OSHA 2009) (Oleari 2015) (Pears 1998)	320–500
Sunrise or sunset on a clear day.	400
Overcast day; typical TV studio lighting (Schlyter 2010)	1000
Full daylight (not direct sun) (Schlyter 2010)	10000–25000
Direct sunlight	32000–100000

Symbols. I: Illuminance.

Note. 1 lm = 1 cd·sr; 1 lx = 1 lm/m2 = 1 cd·sr/m2.

Table 3. Luminance values.

Surfaces illuminated by:	L [cd/m^2]
Moonless, overcast night sky (starlight) (Schlyter 2010)	0.00003
Moonless clear night sky with airglow (Schlyter 2010)	0.00068
Full moon on a clear night (Bunning and Moser 1969) (Schlyter 2010)	0.09 – 0.34
Dark limit of civil twilight under a clear sky (Waynant and Ediger 2000)	1
Family living room lights (Pears 1998)	17
Office building hallway/toilet lighting (AGO 2005)	27
Very dark overcast day (Schlyter 2010)	34
Office lighting (EN 12464-1) (Oleari 2015) (OSHA 2009) (Pears 1998)	109 – 170
Sunrise or sunset on a clear day.	136
Overcast day; typical TV studio lighting (Schlyter 2010)	340
Full daylight (not direct sun) (Schlyter 2010)	3400 – 8500
Direct sunlight	10880 – 34000

Symbols. L: Luminance.

Table 4. Main texture indicators derived

Indicator	Description	Algorithm
MPDiso	Mean Profile Depth measured for wavelengths between 2.5 and 100 mm, according to the Standard (ISO/CD TS 13473-4: 2008) (Praticò and Vaiana 2015) (Riccardi et al. 2016)	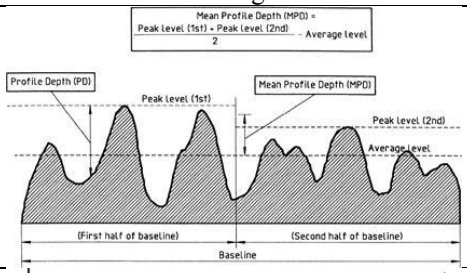
MPD aipcr	Mean Profile Depth measured according to the PIARC algorithm (Boscaino and Praticò 2001).	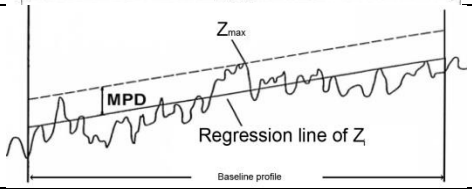
RMS	Root-mean-square roughness (Boscaino and Praticò 2001).	$RMS \approx [\Sigma(Z_i - Z_{average})^2 p(Z)]^{0.5}$
Rz	Average peak-to-valley height (Boscaino and Praticò 2001).	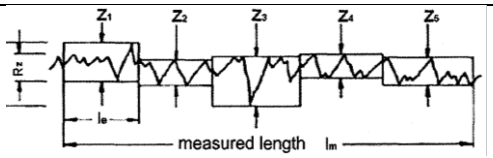 $R_z = \frac{Z_1+Z_2+Z_3+Z_4+Z_5}{5}$
L_t	Texture Level (ISO/CD TS 13473-4: 2008)	$L_{txk} = 10 \cdot Log_{10}\left(2 \cdot \left\lvert \frac{Z_k}{a_{ref}} \right\rvert^2\right)$ for k= 0,…., (1/2N-1) $Z_k = \frac{1}{N}\sum_{i=0}^{N-1} Z_{i,win} \cdot e^{-j\cdot\left(\frac{2\pi k}{N}\right)i}$ for k=0, …, N-1;and j is the imaginary unit (j2=-1) a_{ref} is the reference value of profile amplitude (=10^{-6}m)

Table 5. Timing and quantities (painting process).

Paint	Rate	Duration
	[grams]	[minutes]
WP	17 ± 6	60 ± 5
PP	15 ± 5	30 ± 5

Symbols. WP: White Paint; PP: Phosphorescent Paint; Timing: gap between each laying phase.

Table 6. Model indicators applied to the international literature.

Reference /Sample	a (eq. 7)	b (eq.7)	A=log a	L_{max}	t_1	t_2	$t_2 - t_1$	DS (eq.12)	L_M	PI (eq. 13)
(Bullought et al. 2014) /Steel	425.75	-1.04	2.63	18.40	21	28256	28235	-6.51E-04	0.08	2368
(Bacero et al. 2015) /Board 1	4.02	-0.94	0.60	1.00	4	589	585	-1.69E-03	0.04	25
(Bacero et al. 2015) /Board 2	0.23	-0.26	-0.64	0.48	0	172749	172749	-2.72E-06	0.01	2334

Symbols. a, b: coefficients; Steel: treatment on steel; Board 1: treatment on illustration board-specifications; Board 2: treatment on illustration board; L_{max}: Maximum luminance [cd/m^2]; DS: Discharge slope; t_1: t_2 [s]; L_M: Average luminance; PI: Performance Indicator; Bullough experiments (Bullought et al. 2014) were not carried out on HMA samples.

Figure 1

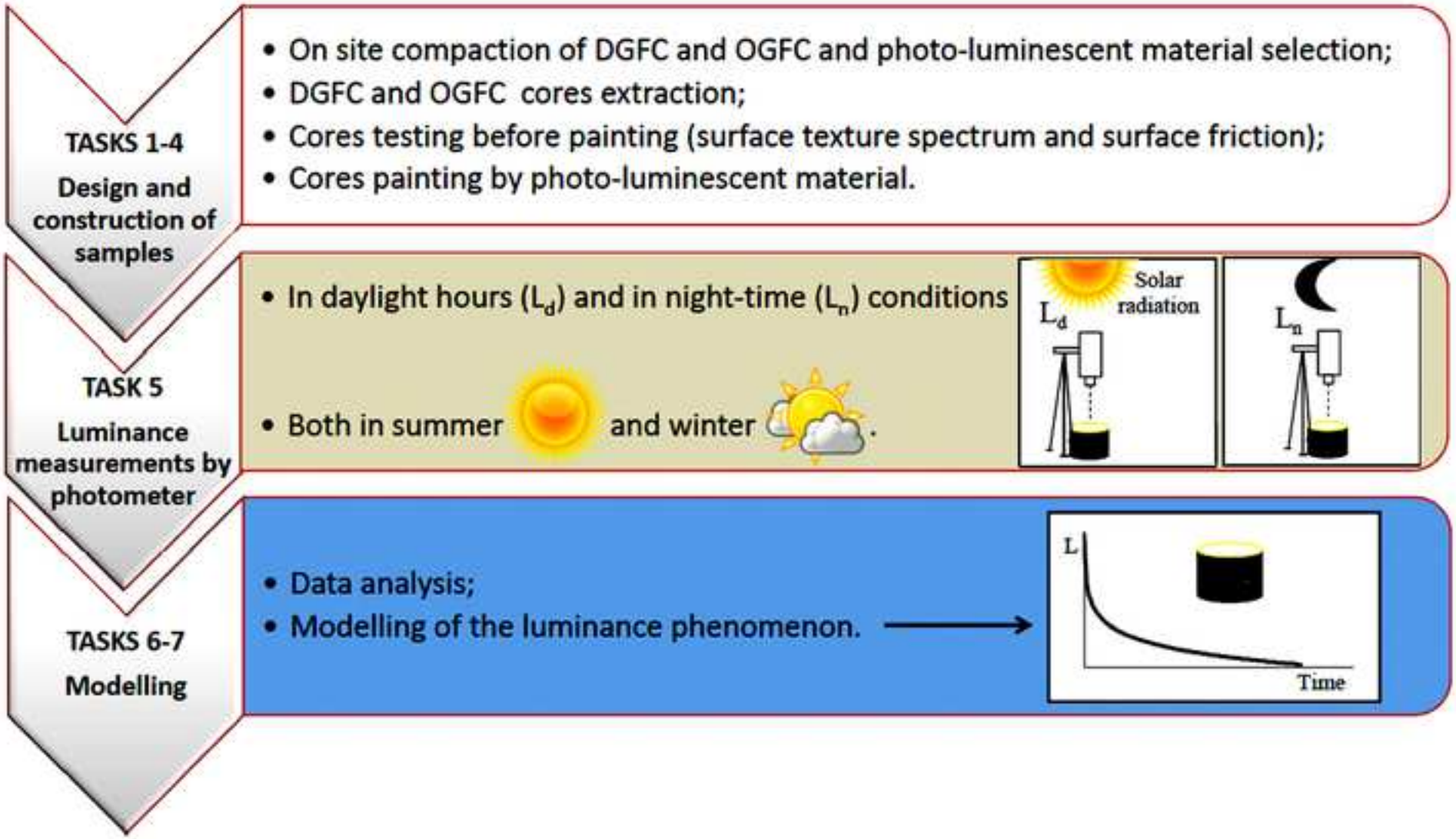

Figure 2

Click here to download Figure Fig2.tif

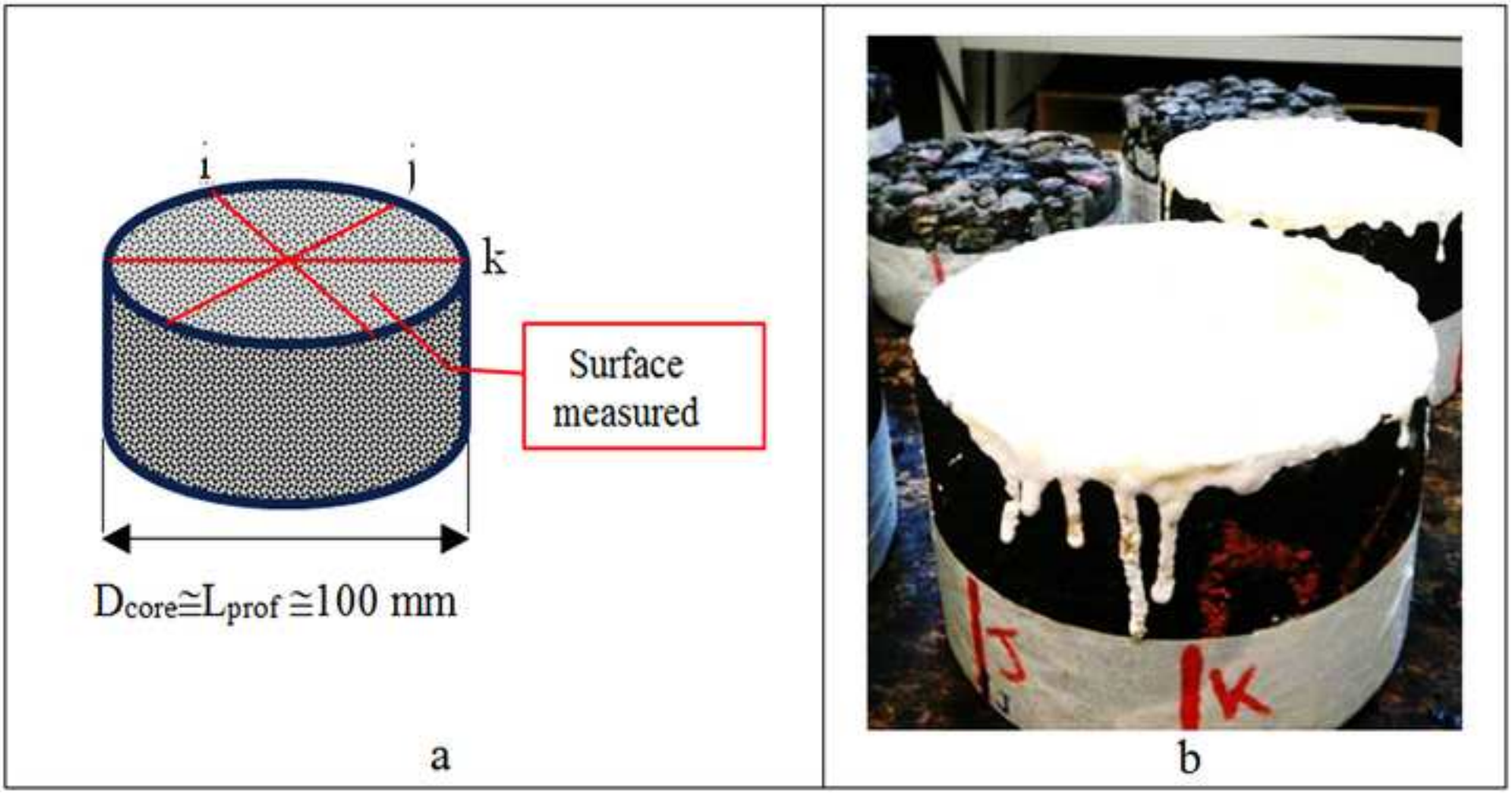

Figure 3

Click here to download Figure Fig3.tif

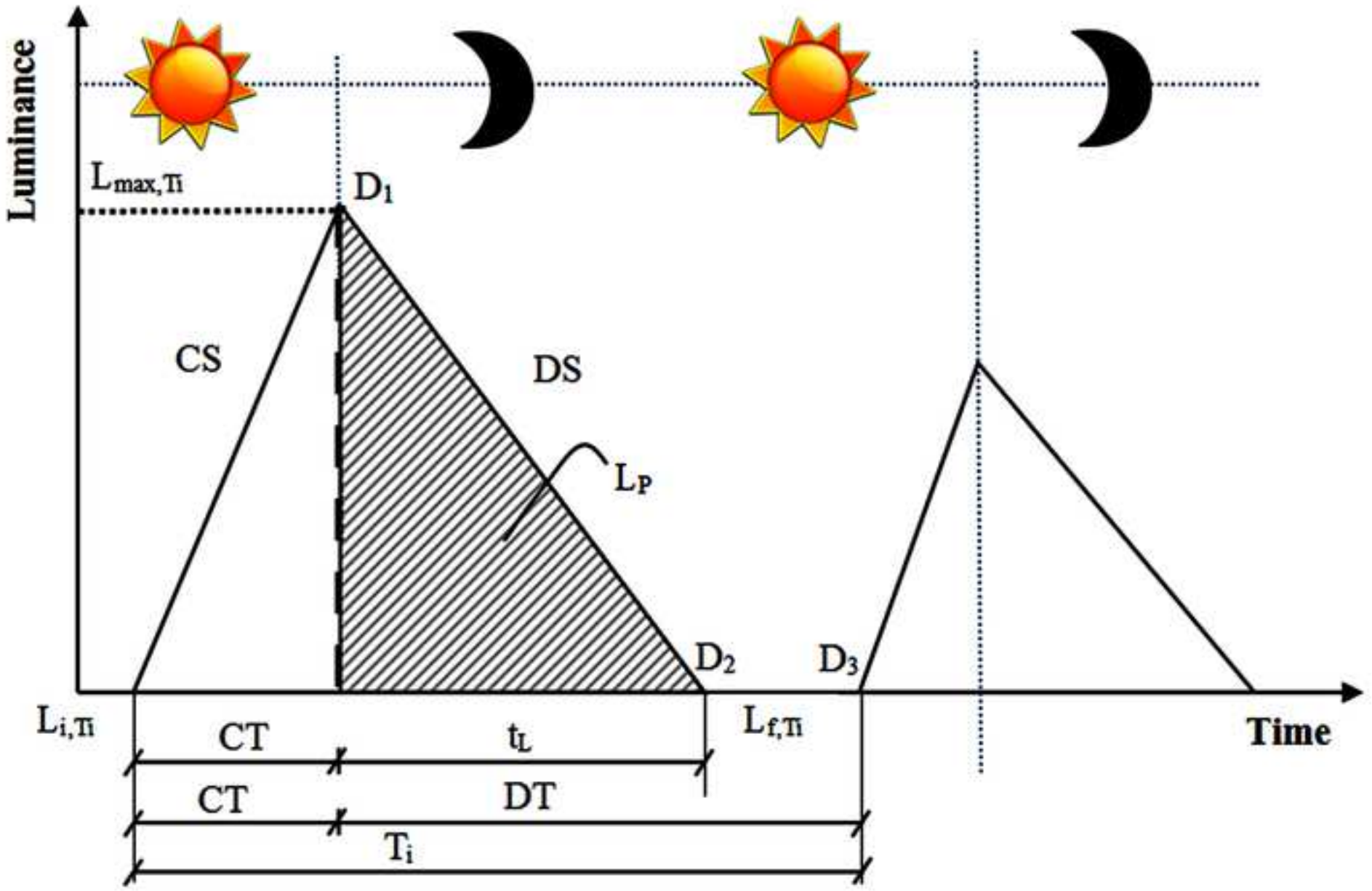

Figure 4

Click here to download Figure Fig4.tif

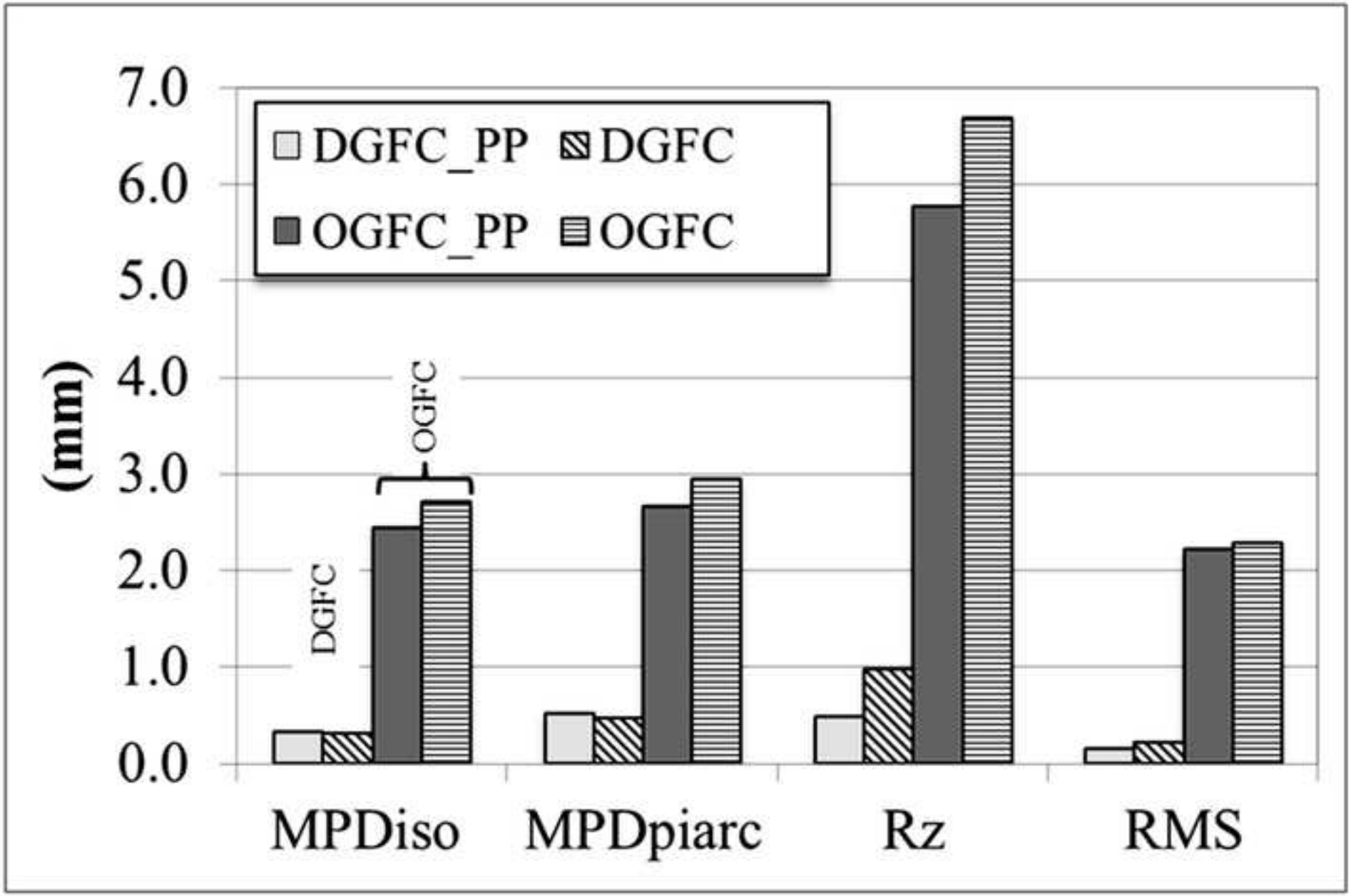

Figure 5

Click here to download Figure Fig5.tif

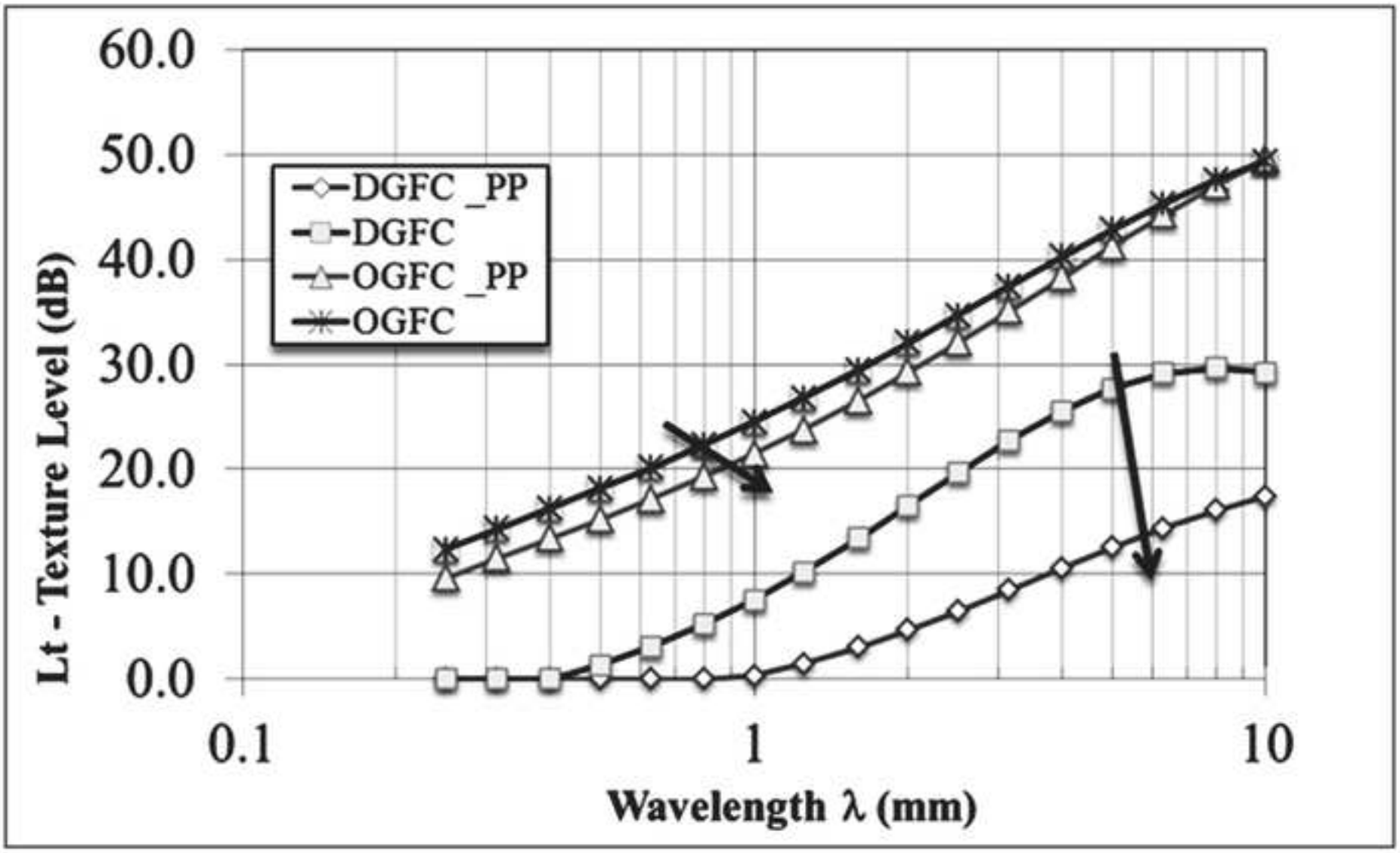

	DGFC	DGFC_PP	OGFC	OGFC_PP
BPN	60	13	54	25

Figure 6

Click here to download Figure Fig6.tif

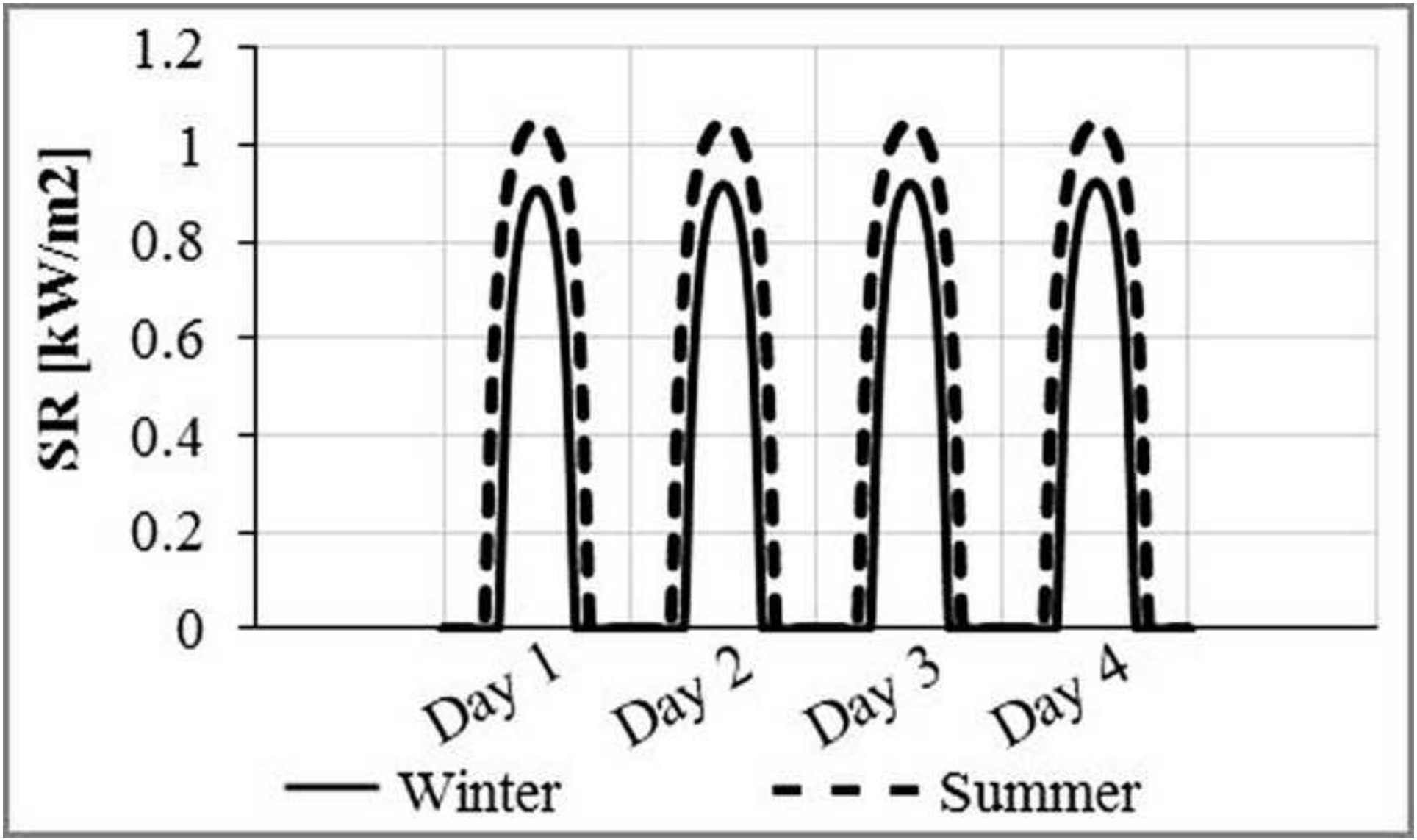

Figure 7

Click here to download Figure Fig7.tif

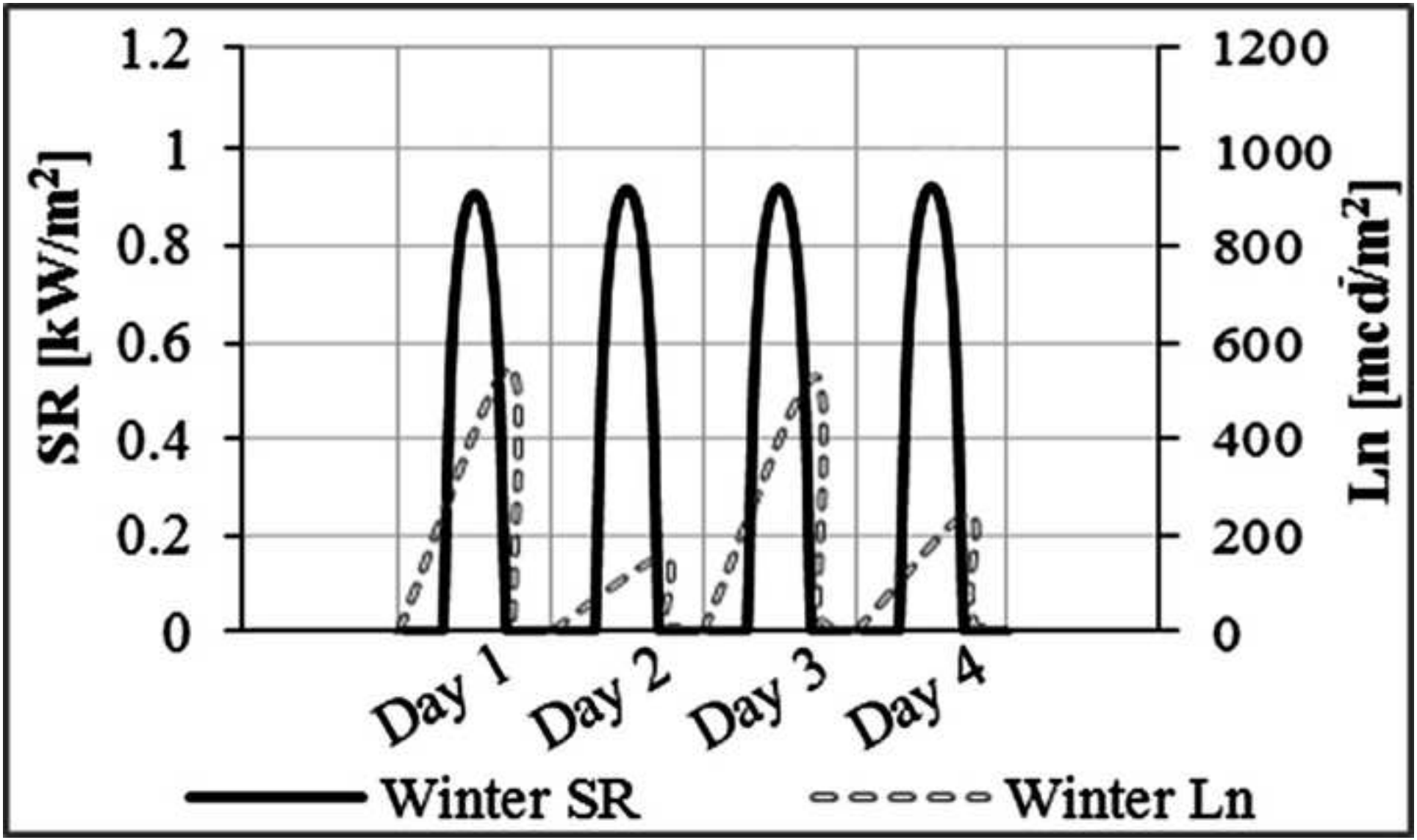

Figure 8

Click here to download Figure Fig8.tif

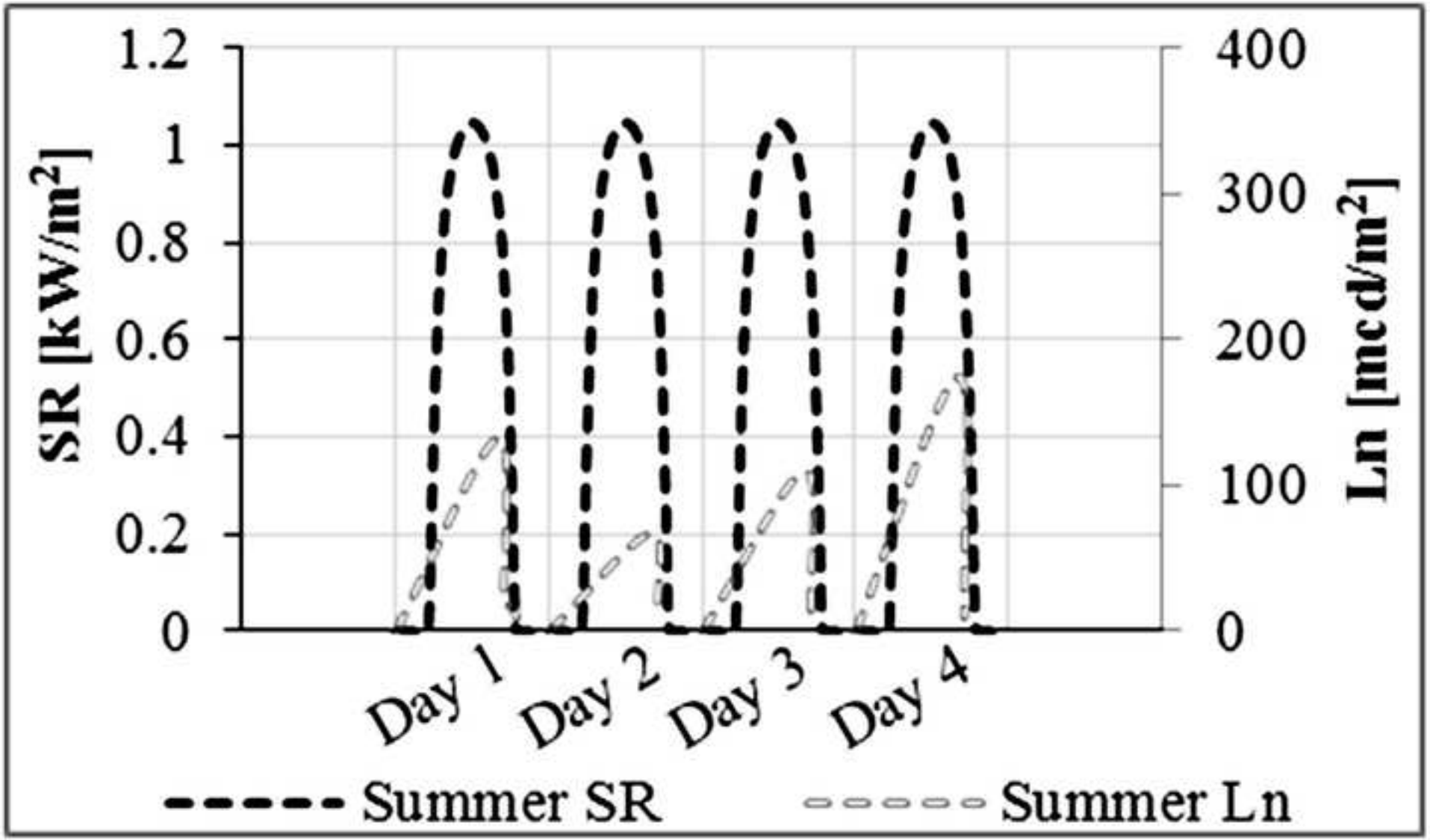

Figure 9

Click here to download Figure Fig9.tif

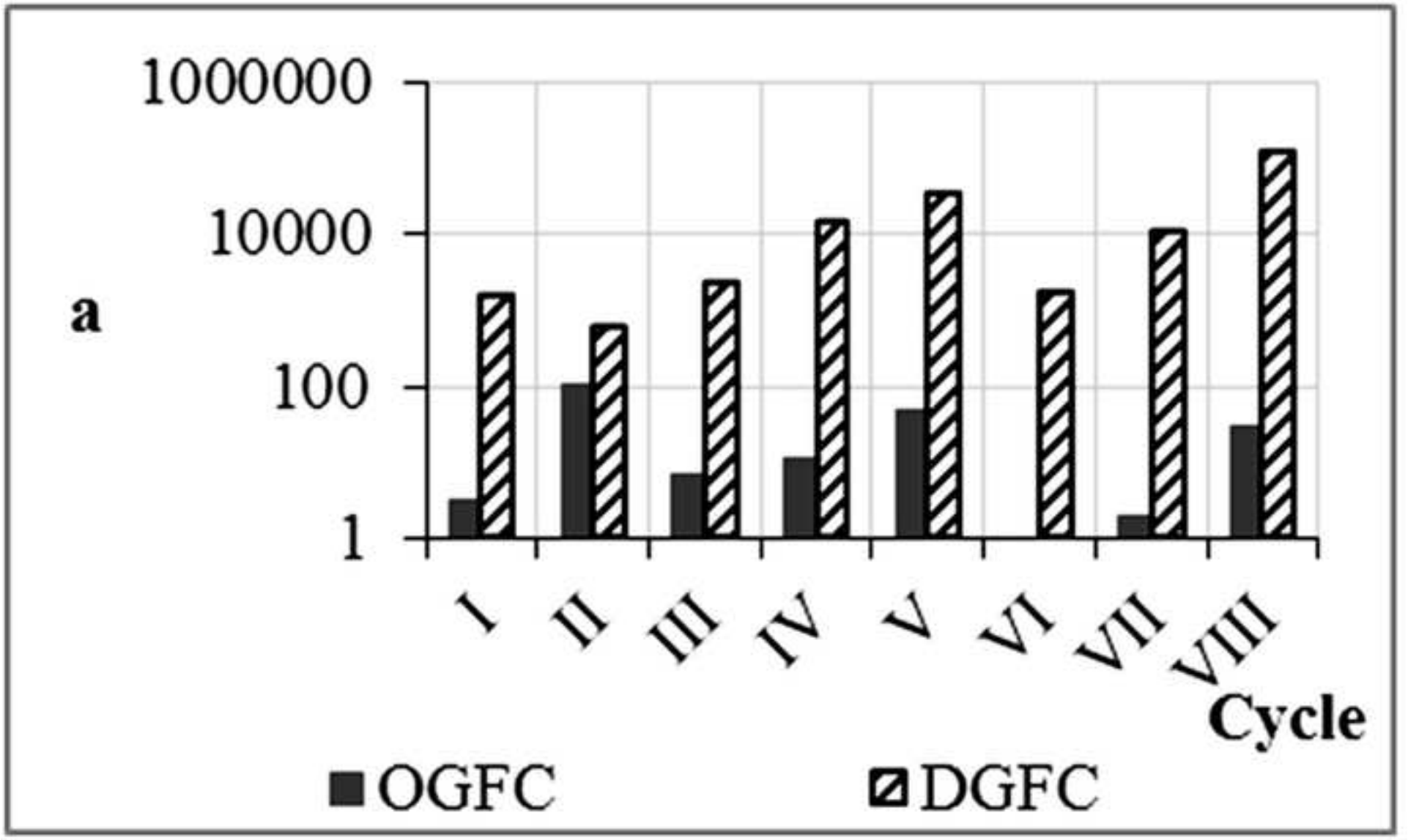

Figure 10

Click here to download Figure Fig10.tif

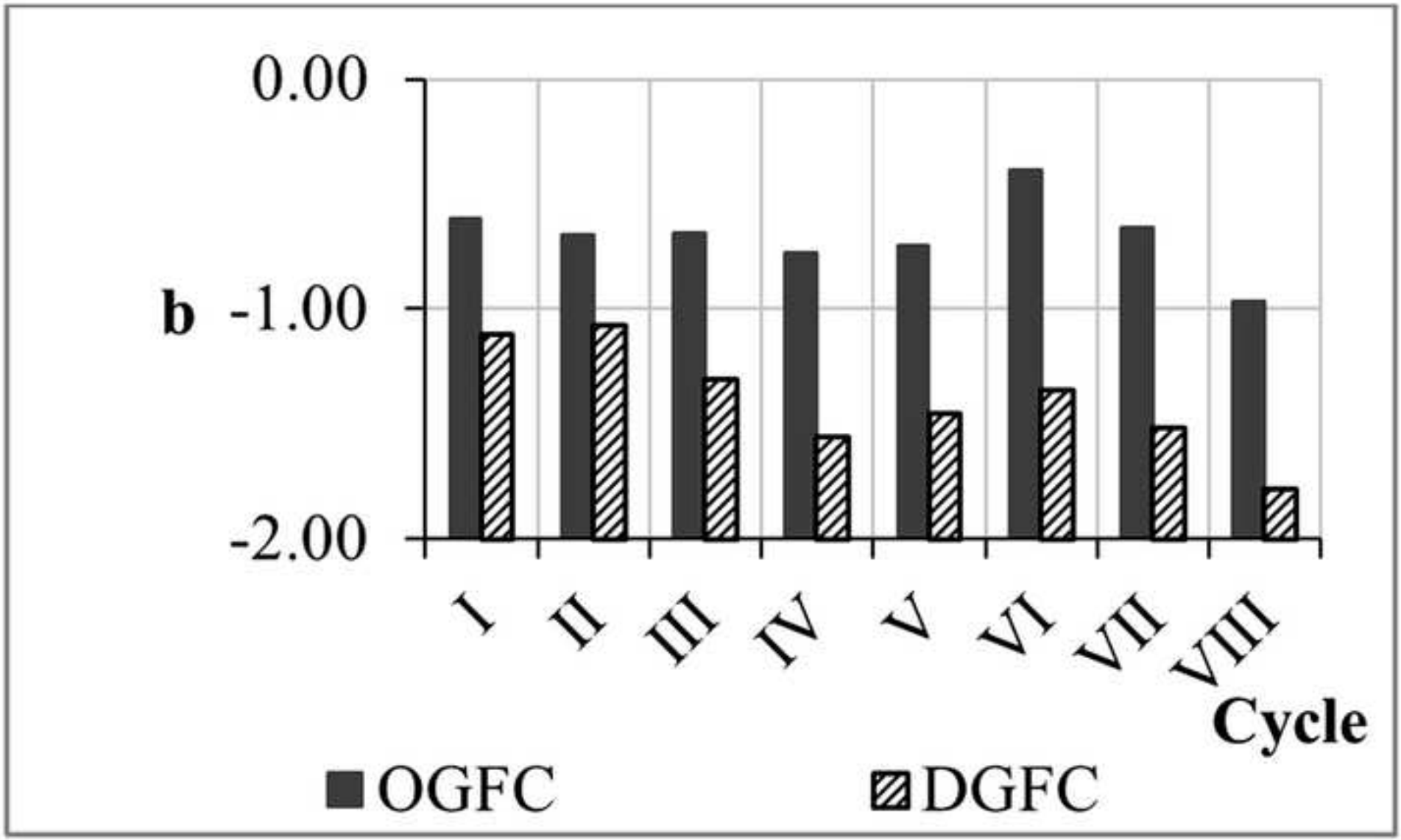

Figure 11

Click here to download Figure Fig11.tif

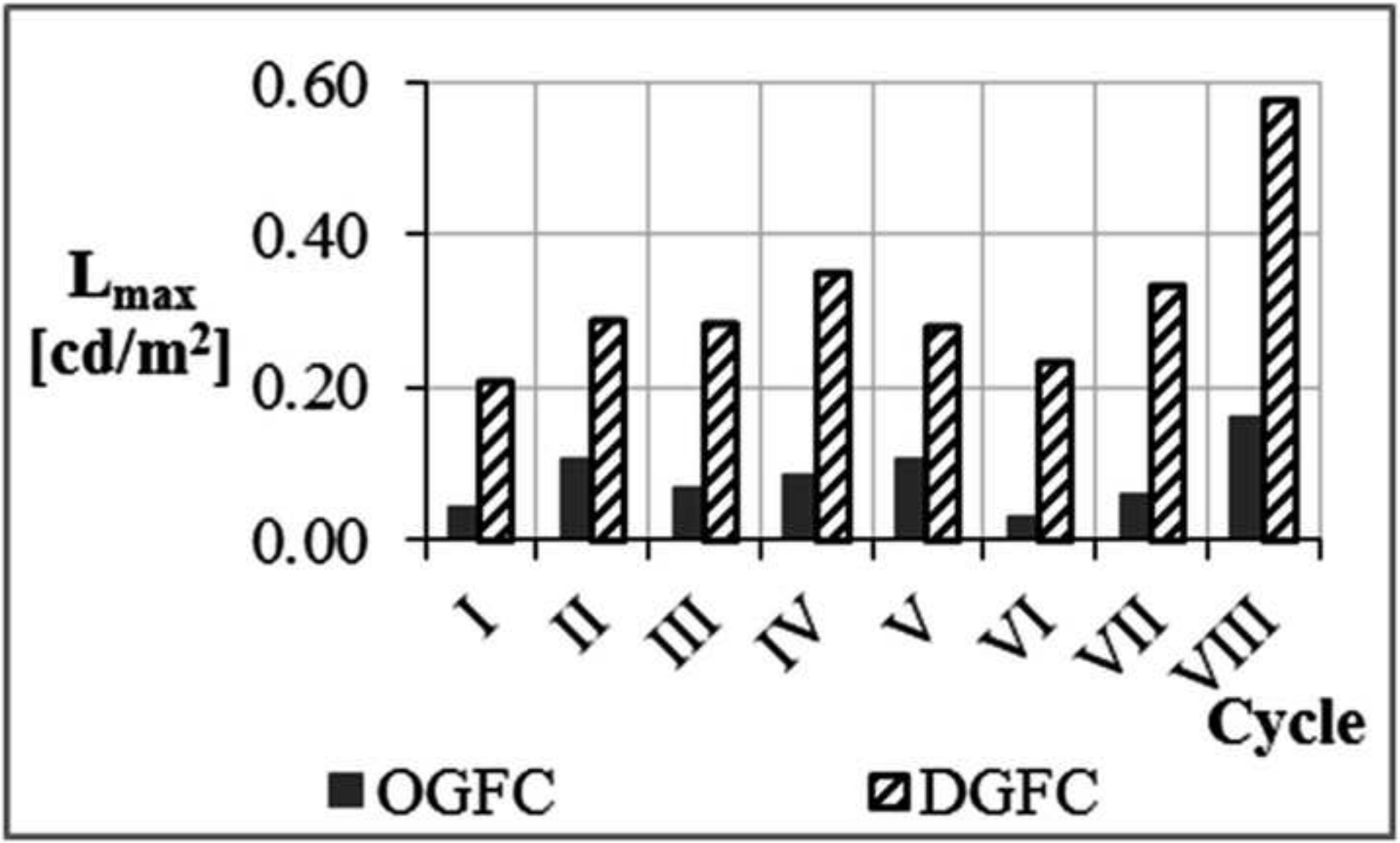

Figure 12

Click here to download Figure Fig12.tif

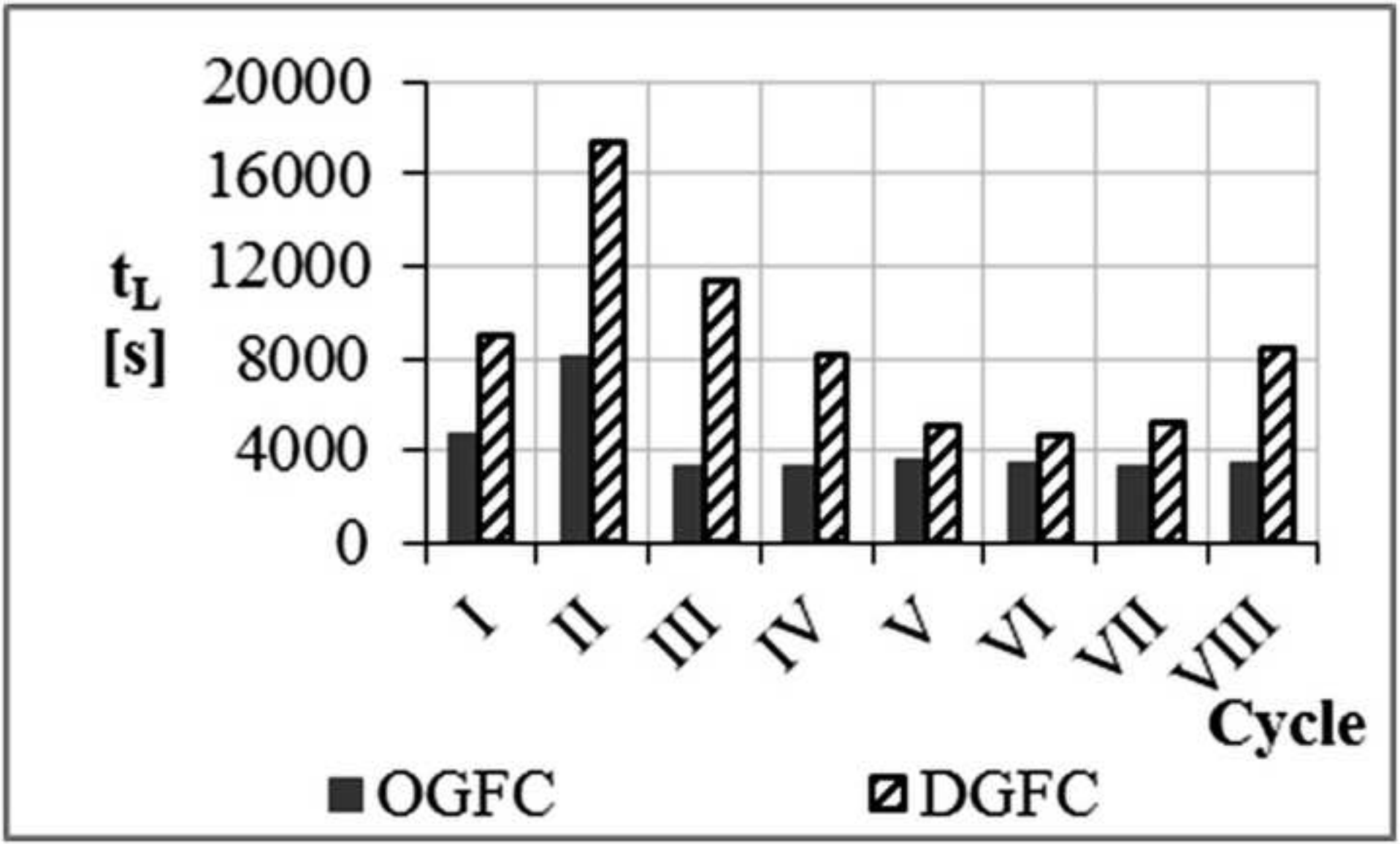

Figure 13

Click here to download Figure Fig13.tif

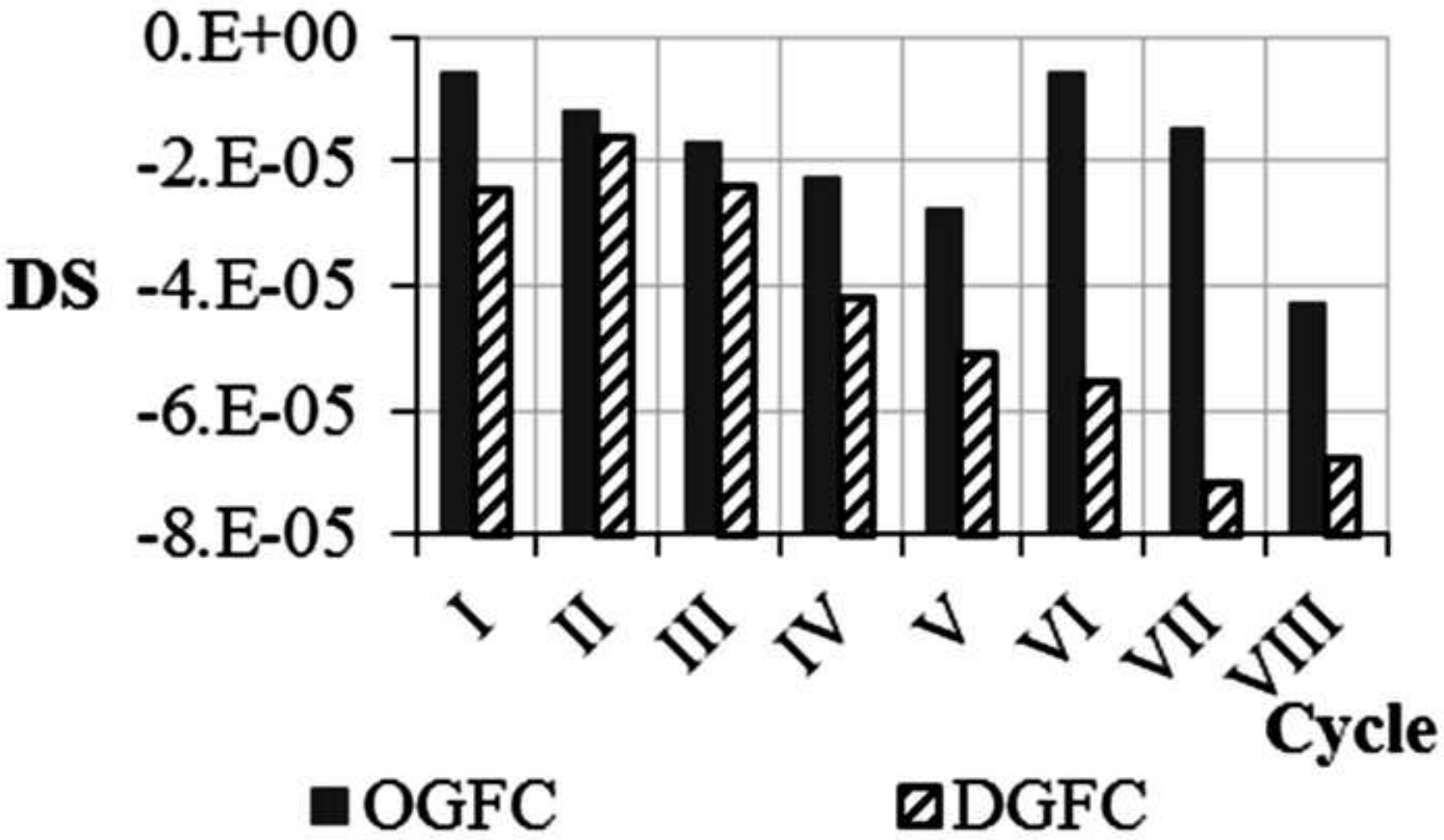

Figure 14

Click here to download Figure Fig14.tif

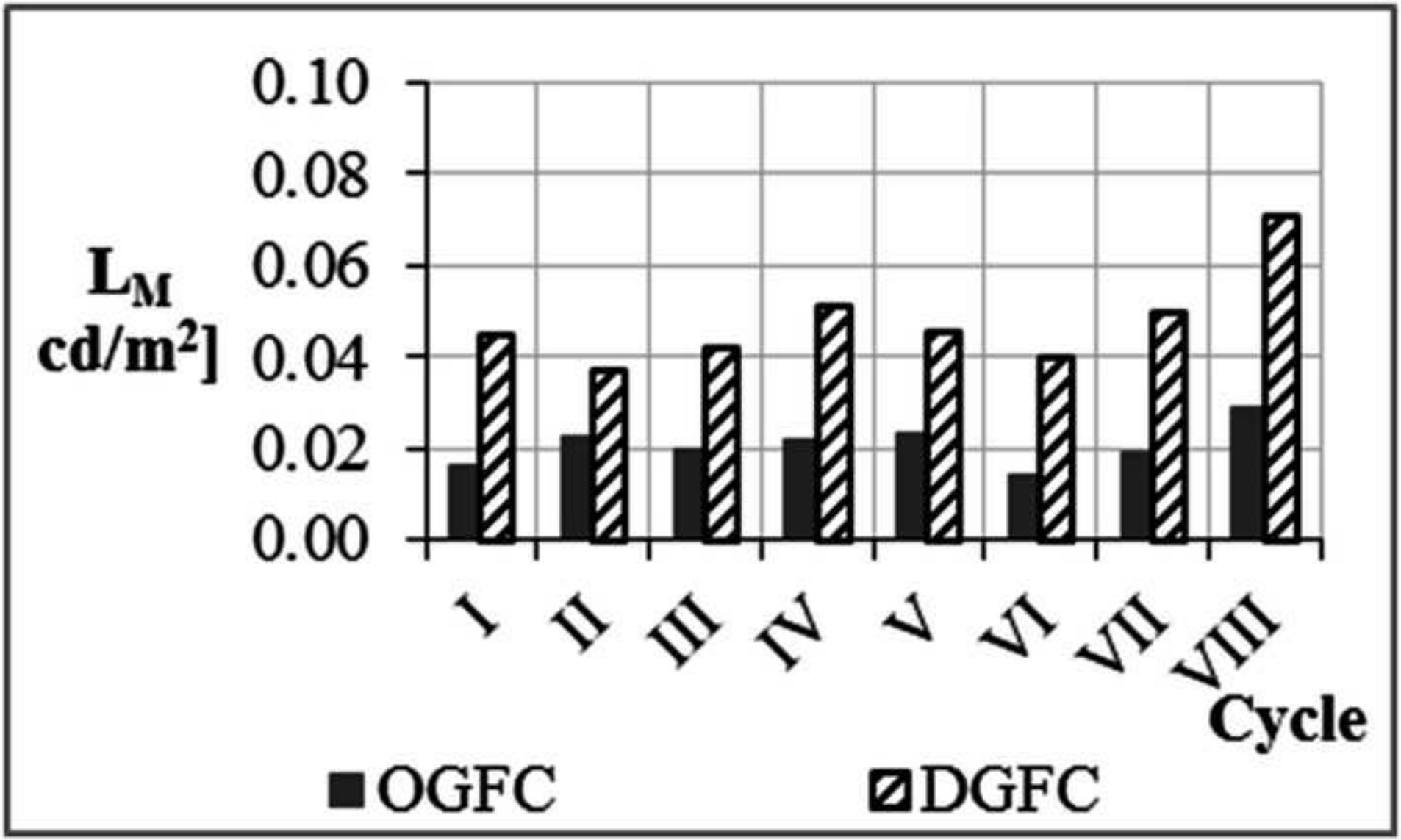

Figure 15

Click here to download Figure Fig15.tif

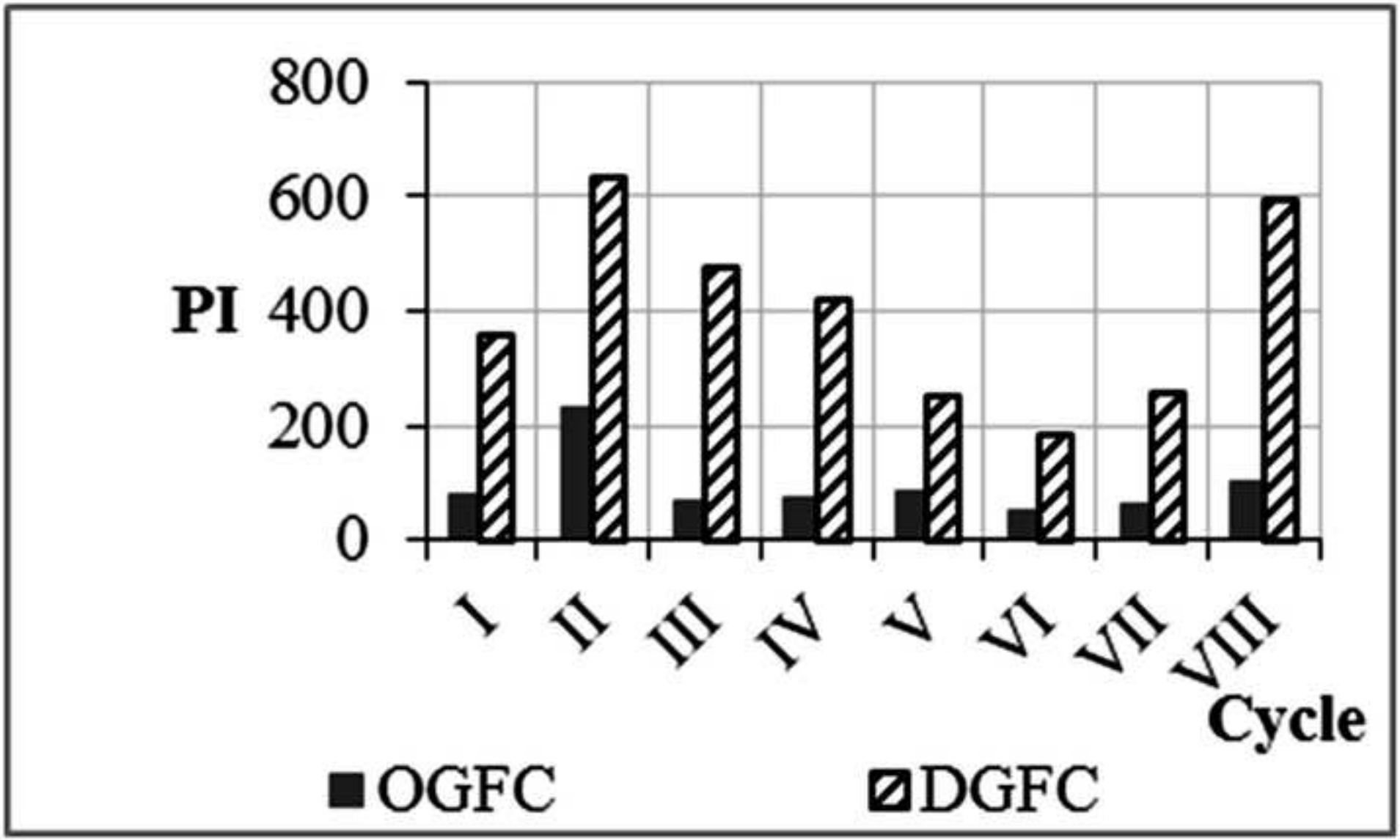

Figure 16

Click here to download Figure Fig16.tif

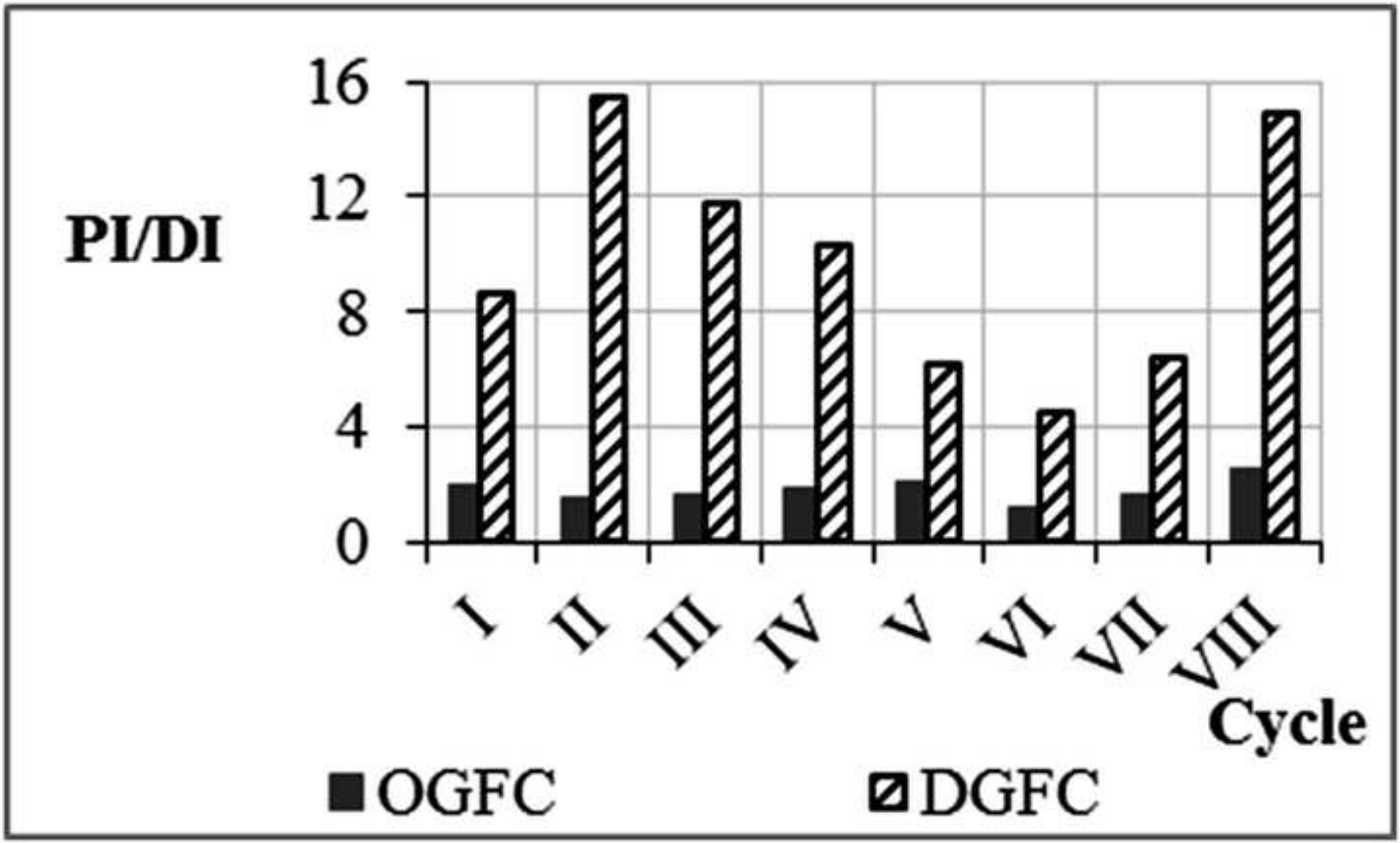

Figure b inside Table 4

Click here to download Figure MPDAIPCR inside Table 4.tif

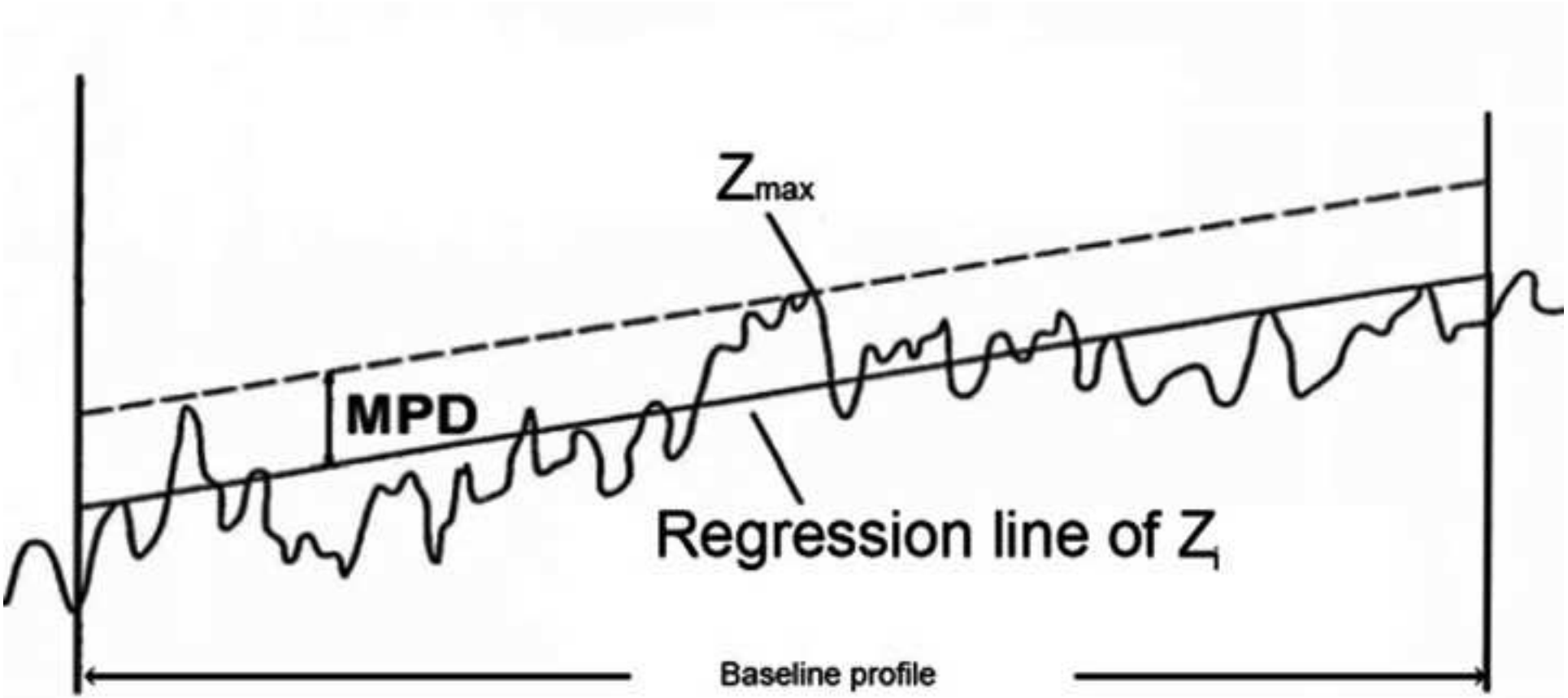

Figure a inside Table 4

Click here to download Figure MPDISO inside Table 4.tif

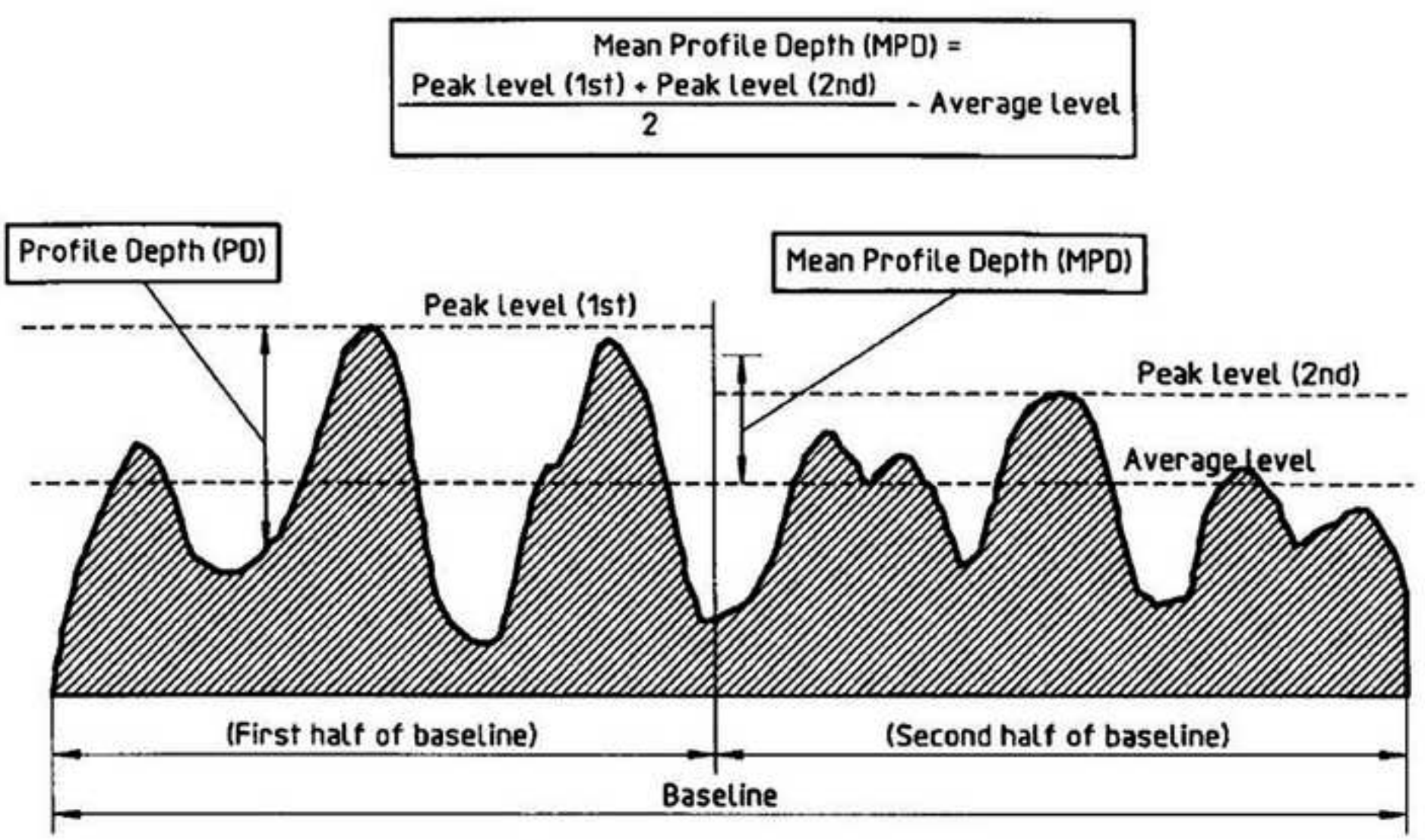

Figure c inside Table 4

Click here to download Figure Rz inside Table 4.tif